

Optical Coatings for Deep Concave Surfaces

Thomas D. Rahmlow, Jr.*^a, Jeanne E. Lazo-Wasem^a, Mark B. Moran^b, and Linda F. Johnson^b

^aRugate Technologies, Inc., 353 Christian Street, Oxford, CT 06478;

^bNaval Air Warfare Center Weapons Division, China Lake, CA 93555

Proc. SPIE 7660, Infrared Technology and Applications XXXVI, 766026 (May 03, 2010);
doi/10.1117/12.850313

Copyright 2019 Society of Photo-Optical Instrumentation Engineers. One print or electronic copy may be made for personal use only. Systematic reproduction and distribution, duplication of any material in this paper for a fee or for commercial purposes, or modification of the content of the paper are prohibited.

Optical Coatings for Deep Concave Surfaces

Thomas D. Rahmlow, Jr.*^a, Jeanne E. Lazo-Wasem^a, Mark B. Moran^b, and Linda F. Johnson^b

^aRugate Technologies, Inc., 353 Christian Street, Oxford, CT 06478;

^bNaval Air Warfare Center Weapons Division, China Lake, CA 93555

ABSTRACT

A method of antireflection coating the interior and exterior surfaces of a deep concave optic is under development and is described. The challenges of coating such an optic include obtaining uniform performance, good mechanical and optical performance across a temperature range of ambient to 1000°C, and the transition to cost effective production. The coating process utilizes a tuned cylindrical magnetron sputtering source which sits inside the nose cone to coat the inner surface and a complementary cylindrical sputtering source to coat the outside surface. The flux from the sputtering source is tuned along the length of the cylinder by stacking an inner core of magnets in such a way as to produce a spatially variant magnetic field which allows the source distribution to approximate a uniform deposition on the surface of the optic. A deposition occulting mask provides fine tuning of source uniformity.

Several magnetron source geometries have been demonstrated. Antireflection coatings were deposited using reactive sputtering. Results are discussed.

Keywords: magnetron sputtering, dome, reactive sputtering, antireflection, concave, optic, optical coating

1. INTRODUCTION

Coating a highly curved, aspheric, and enclosed surface with a high performance anti-reflection film (AR) presents a number of challenges to traditional coating processes. Film thickness must be precisely controlled along the surface. The flux from an evaporation source that approximates a point source, such as an electron beam gun, falls off with the square of distance from the source and with the cosine of the angle of the source to the surface and the angle of the surface normal to the angle of the source¹. While these geometrical considerations can be handled quite effectively when coating flat or slightly curved windows and domes, they are severely limiting for strongly curved and recessed surfaces.

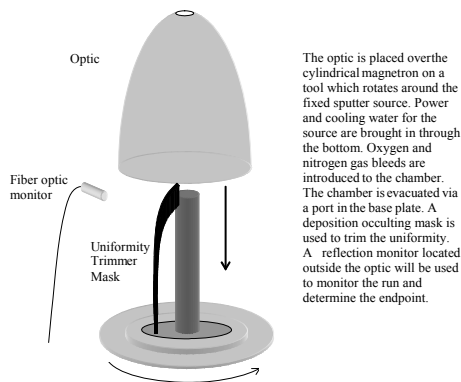


Figure 1: The coating station is modular. The cylindrical magnetron in the center is stationary. The optic is placed over the magnetron on a rotating tool.

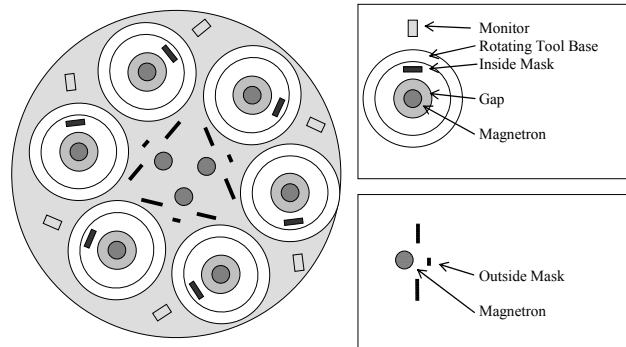


Figure 2: The proposed tooling for coating 6 optics at a time is shown schematically. Nine magnetron sources can be used to coat the interiors and exteriors simultaneously.

The target coating, a six layer discrete design, is a mid-wave anti-reflection film for polycrystalline alumina². The anti-reflection film needs to exhibit high transmission from 3 to 5 μ m over a broad range of angles of incidence. The coating materials must be compatible with high temperature excursions and be stable over long periods of time. The materials

selected for development were Al_2O_3 and AlN . Both materials can be reactively sputtered using an aluminum target, are stable at high temperature, and have coefficients of thermal expansion (CTE) that are similar to the proposed substrate material.

The coating is deposited using tuned cylindrical RF-magnetron sources, as shown in Figures 1 and 2. The optic sits over the magnetron on a rotating platen. Power and cooling water for the source are brought up through the base. The body of the magnetron is aluminum and it doubles as the sputtering target. Reactive gas, either oxygen or nitrogen are added as a background bleed to produce either Al_2O_3 or AlN . The sputtering flux along the length of the magnetron is varied by configuring the internal array of magnets. The process has been demonstrated on fused silica cylinders and on thin glass strips bent to conform to the shape of the concave surface.

The coating station is designed as a module and while only one module has been constructed, it is expected that multiple modules can be installed in a chamber and run simultaneously. Figure 2 presents a top down sketch of six coating stations installed on a single base plate. Exterior magnetrons are included in this sketch for coating the exterior surface of the optics. A provision for adding deposition masks is also shown in the sketch. The deposition masks will be used to fine tune the thickness uniformity of the coating along the optic surface.

A 24" bell jar coating chamber equipped with an 8" cryo pump was used for development. The flow rates of three bleed gasses, Ar, N_2 and O_2 , are controlled using mass flow controllers for each gas. The magnetron source used an Advanced Energy PDX-900 350MHz power supply with a maximum power rating of 900 watts. An Aztech-1000 matching network minimizes reflected power. The cylindrical magnetron coating station is located off-axis. The chamber has a centrally located rotation feed through that is used to provide rotation to the coating station.

A sketch of the cylindrical magnetron coating station is presented in figure 3. The coating station tooling consists of a stationary plate or stand and a set of rotation plates, such that the plate which the optic sits on can rotate about the stationary cylindrical magnetron. Power and water for the magnetron are brought up through the center of the tooling. Figure 4 presents a photograph of the coating station with vertical and curved glass slide holders installed on the rotating plate.

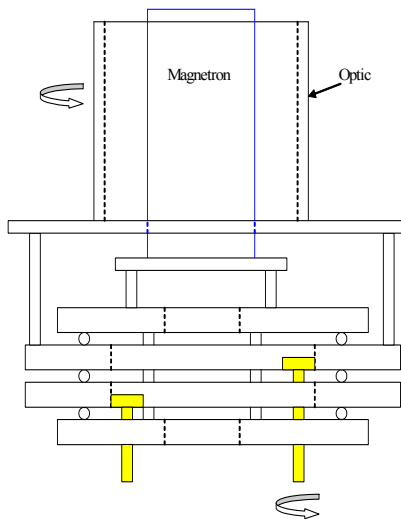


Figure 3: Tooling was designed to rotate cylindrical or deeply concave optics about the cylindrical magnetron during deposition



Figure 4: Aluminum cylindrical magnetron is shown in center of rotating tool, along with curved glass slide holder.

2. MAGNETRON DESIGN

A cylindrical magnetron consists of a metal cylinder filled with an array of rare earth magnets to establish a strong magnetic field around the cylinder. A high voltage is applied to the cylinder, establishing a strong electric field in the space surrounding the cylinder. Charged particles moving in regions where the electric and magnetic fields are perpendicular to each other are deflected into a spiral path. Electrons travel in tight spirals while ionized gas particles move in larger spirals. When the free mean path of the gas is sufficient to support sustained ionization, plasma is established. Gas ions collide with the surface of the cylinder and sputtering occurs. This process is illustrated in figure 5. Cooling water is used to maintain the temperature of the magnetron below the Curie point of the magnets. Water flows up through a tube in the center of the magnet array and flows down the outer wall to the exit tube at the base of the magnetron.

Figures 6 and 7 illustrate the operating states of the cylindrical magnetron. Figure 6 is a photograph of a unipolar cylindrical magnetron (all magnets in the core are aligned with the same polarity) at poor vacuum (50 to 300 millitorr). The rough vacuum is sufficient to support glow discharge, but not sufficient to sustain a significant plasma region. Regions of high electrical stress such as the areas around the screw heads at the top of the magnetron are now glowing. When the vacuum is improved, the free mean path is extended and the collision energies between the free electrons and presented in figure 8, but now operating at 3 millitorr. A strong centralized plasma region is now present.

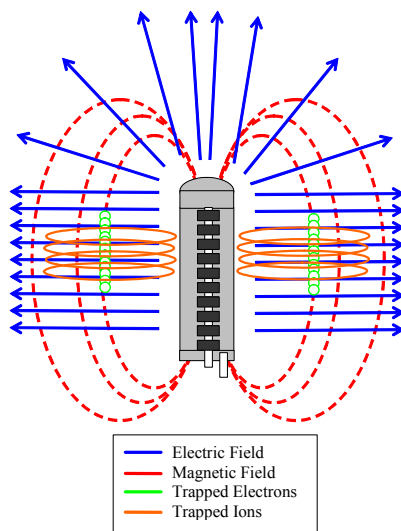


Figure 5: The plasma is generated in the region where the magnetic and electric fields are perpendicular.



Figure 6: In the glow discharge region (poor vacuum) the electric field dominates.

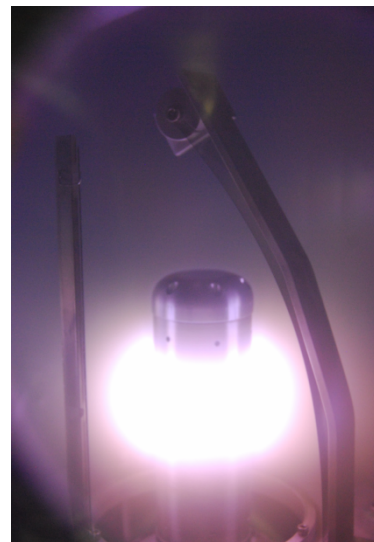


Figure 7: At better vacuum, the ions are trapped and the plasma is enhanced.

The magnets can be arranged in several ways. Figures 8 through 10 present photographs of the plasma with the magnets arranged as a unipolar stack, separated stacks of magnets and sets of magnets with flipped polarity. The unipolar magnet stack exhibits intense plasma in the center of the magnetron. This configuration gives a high plasma rate, but the sputter distribution is unacceptably non-uniform for the present application. The pattern produced by separating the magnets, but maintaining the same polarity (Figure 9), helps improve uniformity, but the sputter rate drops off dramatically. The most practical configuration for the present application is to flip the polarity of adjacent magnet sets. Magnet sets are made up of multiple magnets of the same polarity. Using different numbers of magnets allows for local shaping of the magnetic field strength along the length of the cylinder to achieve good film thickness uniformity on the curved optical surface. Operation of a cylindrical magnetron using the flipped polarity configuration is presented in Figure 10. Each magnet set creates an annular plasma ring.

The magnet configuration developed for coating deep concave surfaces and cylinders is the flipped magnet configuration. The configuration for coating fused quartz cylinders is presented in figure 11. The magnet sets are each

two ½ inch thick neodymium magnets. The polarity of adjacent sets is flipped. Figures 12 and 13 present the assembled magnetron operating with argon/oxygen bleed and argon/nitrogen bleed respectively.

A second magnetron and magnet configuration was optimized for deep concave surfaces. The magnet configuration of this design used magnet sets of 1 to 4 Nd magnets. The magnetic field was varied to meet best uniformity on the concave surface. A challenge in designing the magnetron is getting strong plasma on the nose piece. This sputter region is important for coating the inner tip of the optic. Each plasma ring is electrically in parallel with each other and power is distributed to each circuit accordingly. The solution uses an asymmetric set of magnets near the nose piece to push the plasma up and onto the rounded nose.



Figure 8: Unipolar stacked magnet configuration (UMC)



Figure 9: Separated unipolar magnet configuration (SMC)



Figure 10: Flipped magnet configuration (FMC)



Figure 11: The configuration used for coating cylinders is shown. The polarity of each magnet set is flipped. A final magnet set is three magnets mounted in the nose piece.



Figure 12: Each flipped pair creates a plasma ring. The bleed gases are argon and oxygen.

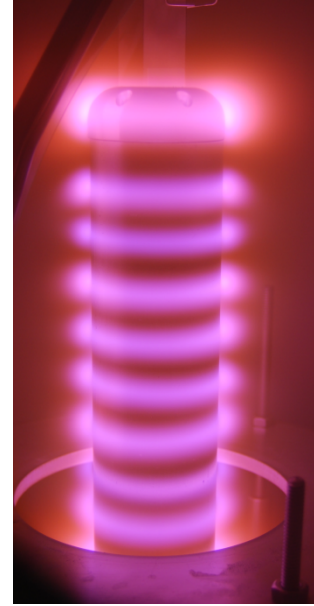


Figure 13: Nitrogen rich glow. The unbalanced magnetic field at the top pushes the final plasma ring up onto the nose piece.

3. METROLOGY

Two test tools were developed to characterize coating thickness uniformity. These tools each hold a glass strip 1" wide and 9.25" long. The glass used is less than 200 μm thick and is easily deflected into a curve mimicking the shape of the ogive. The glass strips were also mounted vertically to mimic the wall of a cylinder. These glass strips were typically included in each test run to characterize changes made to the cylindrical magnetron or process parameters.

A motorized test stand was assembled to map performance along the glass strips. The test stand was operated under computer control. When aluminum films were deposited, the strips were characterized for optical density. Measured optical thickness was compared to the modeled optical density of aluminum and these measurements were then converted to film thickness. When the films were either Al_2O_3 or AlN , a visible transmission spectrum was acquired and the transmission scan was iteratively modeled to calculate optical thickness. In each case, the glass strips were mapped along the length of the glass. The typical measurement interval along the glass was 0.5". Figure 14 presents a sketch of the glass slide monitor.

In addition to measuring optical performance, the motorized test stand was also fitted with an array of Hall Effect sensors. This array allowed the measurement of the magnetic field over the length of the magnetron. The height of the array could be lifted and was used to map field strength both along the cylinder axis and perpendicular to the axis.

Run to run stability in single film thickness was better than 5% based on power and sputter time for similar process values of power, chamber pressure and gas bleed rates. However, in situ monitoring and feedback is needed to achieve high film quality and optimal transmission. Initial work performed to date on in situ metrology includes plasma monitoring for gas composition and the addition of fiber source and pick-off probes on the witness slides. Figure 15 presents measured plasma spectra for argon, oxygen and an argon/oxygen gas blend.

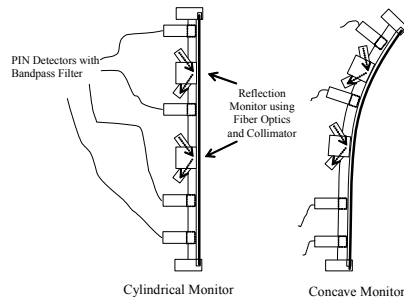


Figure 14: The witness slides

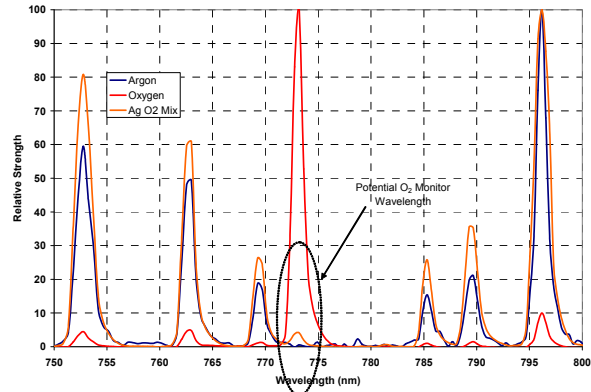


Figure 15: Measured spectrum for the argon and the oxygen plasma are overlaid to identify potential spectral lines for process monitoring.

4. COATING DEMONSTRATION

Coating demonstration consists of demonstrating film uniformity, film quality, characterization of dielectric films, coatings on curved and vertical surfaces and anti-reflection coating on confined surfaces (specifically cylinders). Gas ratios and chamber pressure set points were not optimized. Process development was limited to finding an acceptable set of ‘baseline’ parameters. Table 1 lists the baseline process conditions.

Film uniformity was initially characterized following a change in magnetron design by making a 1 to 5 minute aluminum test run. Glass samples mounted in the vertical and concave witness holders were characterized for optical density. The optical density was converted to film thickness using modeled transmission as a function of film thickness. The film thickness was then normalized to the maximum measured thickness. Figures 16 through 18 present the optical density to film thickness function and an example thickness distribution curve for the unipolar magnet stack.

Samples of dielectric films were fabricated and characterized for thickness uniformity, optical properties and film quality. Optical thickness was calculated by modeling measured visible scans made along the glass strips. The optical thickness was then used to calculate film uniformity. Vertical and concave shaped glass strips were typically coated in each run prior to the cylinder test runs. Once cylinder deposition testing was begun, only vertical strips on the wall of the cylinders were included in each test run.

Table 1: Baseline Test Parameters

Base pressure prior to start:	< 4.0 10 ⁻⁵ torr
Chamber pressure during run:	4-5 10 ⁻³ torr.
Pre-run conditioning:	100 watts, argon/O ₂ bleed
Single Layer Tests:	Al films: 1 to 5 minutes at 500 to 900 watts. Al ₂ O ₃ films: 180 minutes at 800 watts AlN films: 120 minutes at 800 watts
MSC Set points:	Al Films: Ar: 4.01 Al ₂ O ₃ films: Ar 4.01; O ₂ 0.65 AlN films: Ar: 1.01; N ₂ 9.01
Cylinder wall temperature:	160° C after preconditioning, 310 - 330° C after 15 minutes coating
Test film thickness:	Al films 120 to 1200 Å
Test film rates:	Al ₂ O ₃ 0.92 Å/sec AlN 1.64 Å/sec

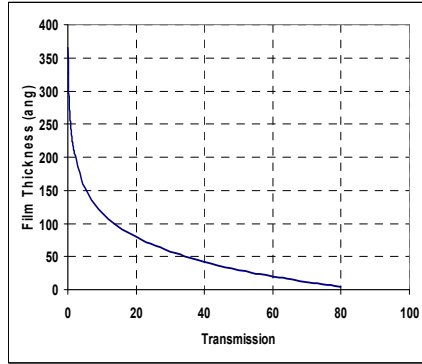


Figure 16: Modeled transmission through the metal film at 540 nm is used to convert from measured transmission to film thickness.

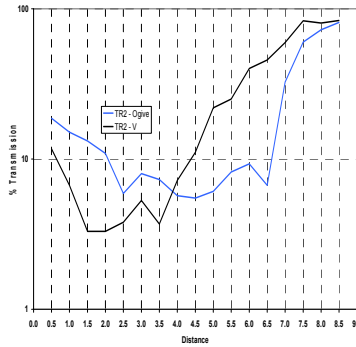


Figure 17: Transmission is measured at 540 nm using a laser OD tester.

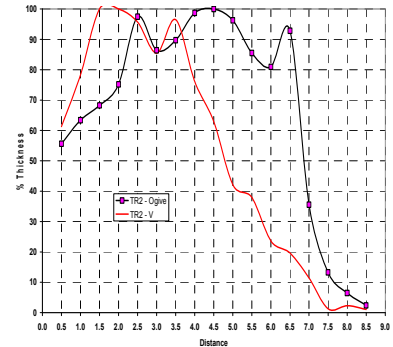


Figure 18: Transmission measurements are converted to film thickness

5. RESULTS

Technical development was driven by two target geometries. These geometries are a 5” diameter by 7.5” high cylinder and a 1.5 caliper ogive with a deeply concave optic of the same diameter and height. The two geometries were sufficiently different to require that a cylindrical magnetron be configured for each target optic. The cylindrical magnetron developed for the cylinder is 10” tall. Its magnet array consisted of 11 pairs of magnets with flipped polarity. The cylindrical magnetron developed to coat the concave optic was 5.75” tall. The six magnet sets were configured using an asymmetrical distribution to correct for changes in deposition thickness along the curve. The final magnetron design for coating the concave optic is presented in Figures 19 through 22.

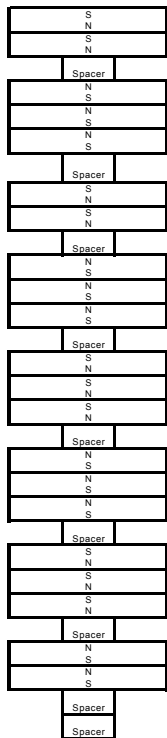


Figure 19: Magnet Assembly

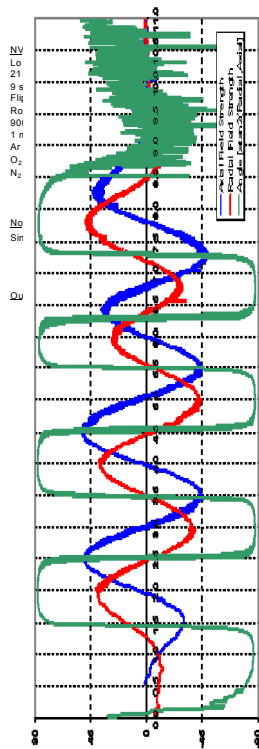


Figure 20: Magnetic Field



Figure 21: Argon Plasma

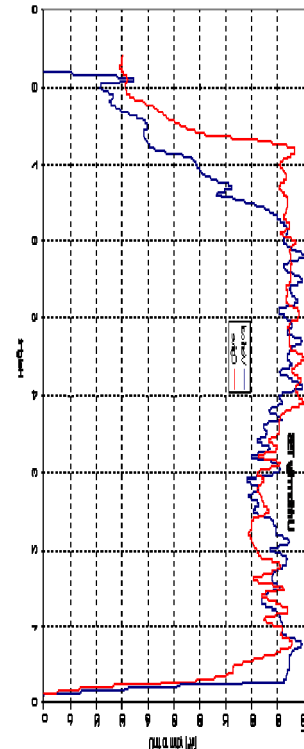


Figure 22: Measured Uniformity

In both cases, adequate uniformity was achieved along the surface to allow for final adjustment with a deposition mask. Future work on improving the sputter rate of the nose piece will be needed to improve uniformity for the upper 1" of the interior of the optic if it is necessary to coat that region. Figure 23 and 24 present measured uniformity for the two cylindrical magnetrons on their target surfaces.

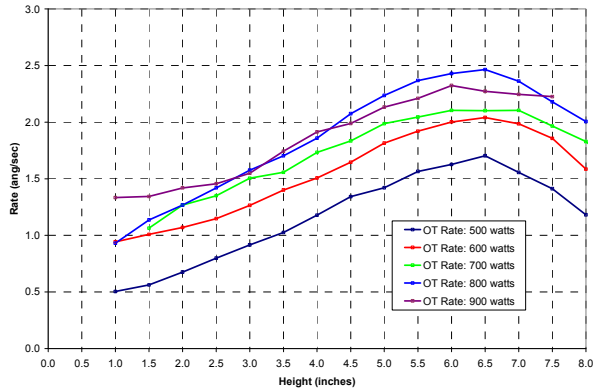


Figure 23: Measured uniformity on the 5" diameter cylinder using the 10" cylindrical magnetron.

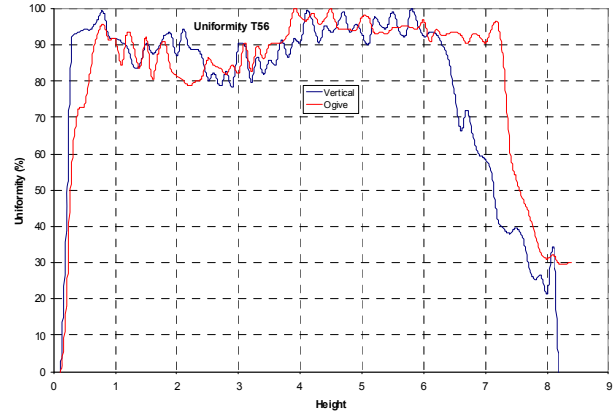


Figure 24: Measured uniformity on the target ogive of the 5.75" cylindrical magnetron. The red line is the uniformity on the ogive shaped slide. The blue line is uniformity on the vertical slide.

Figure 25 through 27 present measured deposition rates as a function of magnetron power. Figure 25 presents the measured rate at the height of 6" in the cylinder for both the oxide and nitride as a function of magnetron power. The oxide rate is less than half the rate of the nitride. Figures 26 and 27 present deposition rate as a function of height within the cylinder measured from the cylinder's base.

Three 6-layer ARs were deposited on fused quartz cylinders. Spectral scans for the ARs on 1" sapphire samples are presented in figure 29.

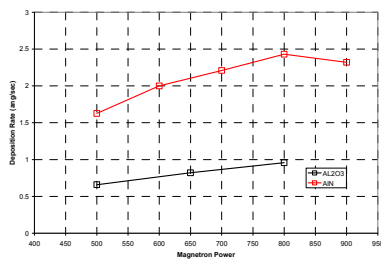


Figure 25: Measured optical thickness (OT) disposition rates at a height of 6" in the cylinder for Al₂O₃ and AlN are plotted as a function of magnetron power.

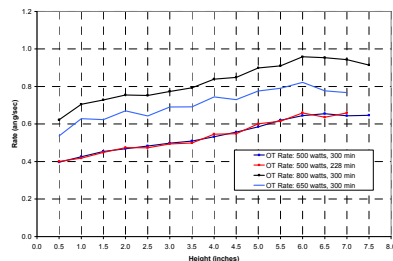


Figure 26: Measured optical thickness rate (Å/sec) for Al₂O₃ films deposited on glass strips attached to the wall of a cylinder using the 10" cylindrical magnetron.

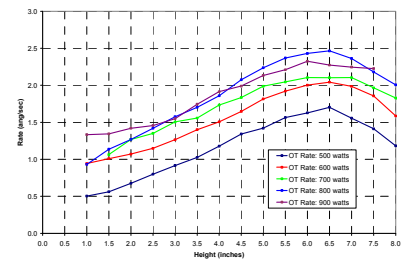


Figure 27: Measured optical thickness rate (Å/sec) for AlN films deposited on attached to the wall of a cylinder using the 10" cylindrical magnetron.



Figure 28: The back cylinders are coated with a single film of AlN (left) and Al₂O₃ (right). The front cylinder is coated with the 6-layer AR design. It has a light yellow tint due to some absorption in the visible. The films exhibit good adhesion and film quality.

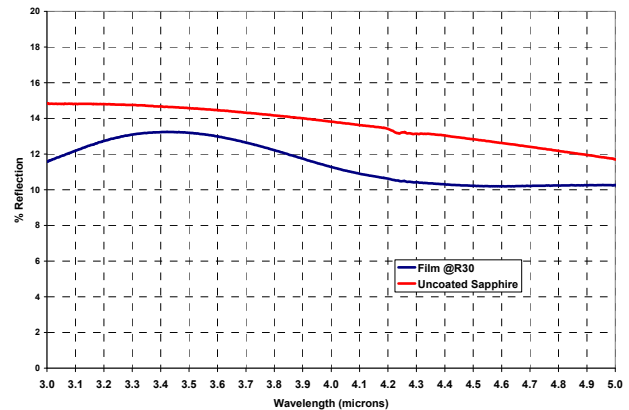


Figure 29: Measured reflection at 30° AOI for a sapphire substrate coated with the AR design on a single surface is plotted along with measured transmission for an uncoated substrate.

6. CONCLUSIONS

The goal of this effort was to prove the feasibility of using a cylindrical magnetron and reactive gas sputtering as a means of coating deep concave surfaces. The work was driven by two target geometries specified in the statement of work: a 5" diameter, 7.5" tall cylinder and a deeply concave optic of the same diameter and height.

Initial work focused on configuring the magnet array of the cylindrical magnetron to produce good, first order deposition uniform on witness glass slides deflected into the shape of the deep concave target surface. A high degree of uniformity was achieved from the base to a distance along the surface of 7.5". Further work will be needed to extend deposition another inch or so in to the nose of the optic, but uniformity results on the concave surface are sufficient to achieve a high quality precision optical coating on the inner surface.

Following demonstration of thin film uniformity control on the deep concave surface, the focus of work was readdressed to demonstrating that the cylindrical magnetron was capable of depositing the desired optical coating in a confined space without detriment to film quality. This was demonstrated by coating the interior of 5" diameter cylinders. The cylinder wall temperature was measured in excess of 300 degrees during the coating and the plasma visible extended to the cylinder walls. However, the quality of the deposited films was very good. No pitting or etching of the surface of the films is observed. The optical performance of the AR films needs further development and process optimization, but film quality, adhesion on the cylinder and uniformity of performance are all well demonstrated.

The use of the cylindrical magnetron for coating high quality antireflection films on deep concave surfaces was demonstrated and is practical. Further development work will address process optimization and improve optical performance.

REFERENCES

1. Macleod, H., *Thin-Film Optical Filters*, 3rd edition, IOP Press, (2001)
2. M. V. Parish, M. R. Pascucci, "Polycrystalline alumina for Aerodynamic IR domes and windows", Proceedings of SPIE Vol. 7302 (2009)